FACTORS INFLUENCING DEVELOPMENT, UTILITY AND NEW DIRECTIONS IN MEDICAL IMAGING:

FROM MAGNETIC RESONANCE TO X-RAYS

Jenghwa Chang and Randall L. Barbour

Department of Pathology, SUNY Health Science Center at Brooklyn

450 Clarkson Avenue, Brooklyn, NY 11203

I. INTRODUCTION

Imaging studies are finding increasing applications in clinical medicine. Fueling this have been advances in technology that have expanded the range of applications and have improved their clinical performance, (*i.e.*, diagnostic sensitivity and specificity). In addition, in many cases the risks associated with imaging procedures are minimal. The combined effect has been a tilt in the cost-benefit balance in favor of expanded use. Recent economic pressures, however, are adding increasing weight to cost considerations, requiring many to rethink their approach to the development of improved or fundamentally new imaging technologies. In this report, we examine some fundamental and practical issues that can be expected to influence future development of imaging technologies. We also discuss approaches that we are taking to develop NIR imaging methods, which we believe have significant potential for improving the performance for certain applications while maintaining high cost-effectiveness.

Medical Imaging Using Electromagnetic Radiation

Electromagnetic radiation has been explored for its medical diagnostic and therapeutic applications since the discovery of x-rays by Wilhelm Röntgen in 1895. Since that time, a variety of imaging modalities have been developed that employ energy sources which operate in different regions within the electromagnetic spectrum. Source frequencies that have been successfully adopted range from close to DC, up to ultrahigh frequencies associated with gamma rays, all of which travel at velocity c in a vacuum. Depending on which form is employed, the information derivable can be mainly anatomic or functional in nature. Which of these are emphasized depends on the type of energy-tissue interaction and on a host of practical issues. In Figure 1 the frequency, wavelength, and photon energy of the radiation associated with various medical imaging applications are indicated.

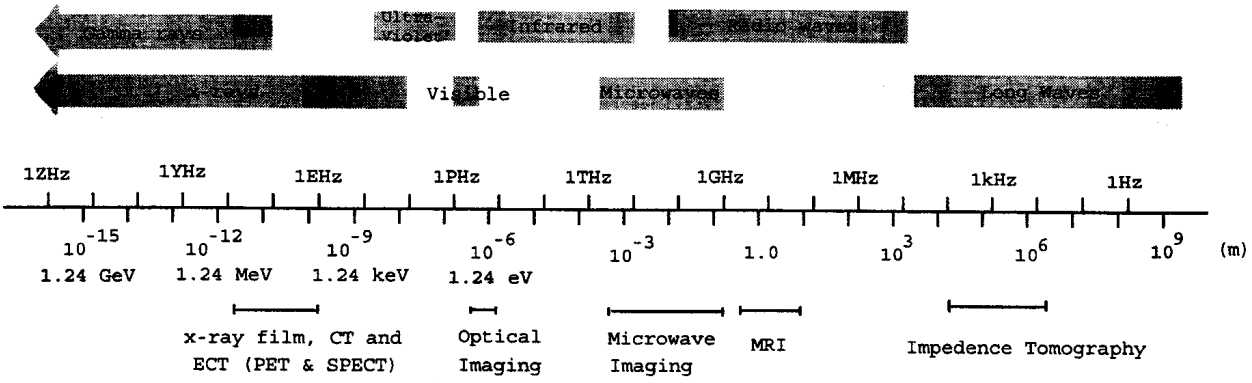

Figure 1. The Electromagnetic spectrum .

Common to all imaging technologies is the need to employ a form of penetrating energy, and the importance of considering factors that influence contrast, resolution (both temporal and spatial) and sensitivity.

i. Penetration: Factors influencing penetration include absorption and scattering. The combined effect of these is usually referred to as *attenuation*. A necessary condition for penetration is that, absorption must be small at the

SPIE Vol. 3171 • 0277-786X/97/$10.00

chosen wavelength. Within the electromagnetic spectrum, there are three regions where this condition is met. These include frequencies below 10 GHz ($<10^{-5}$ eV), between 200 and 500 THz (NIR region, ~1 eV), and above 10^{18} Hz (x-ray, gamma ray region, >10 keV). At frequencies between 10^{10} and 10^{18} Hz, with the exception of the NIR-UV region, penetration into tissue is greatly restricted, mainly by absorption by water. In tissue, energy penetration is further restricted to NIR wavelengths because of strong absorption by hemoglobin in the visible range, and by proteins and nucleic acids, among others, in the UV region. While appreciable penetration (multi-centimeter) can occur in the indicated spectral regions, the wavelength ranges appropriate for medical imaging are further limited, primarily as a consequence of insufficient contrast in the case of low frequency sources, and of limits on exposure to ionizing, or high energy, sources. Spectral regions where imaging applications have been identified include x-rays in the 10-150 keV range (x-ray imaging), gamma rays in the 100-500 keV range (SPECT, PET imaging), the RF region in the presence of a large external magnetic field (MRI) and electric sources operating below 10 kHz (impedance imaging). In the RF and high energy regions, imaging is favored by weak scattering. Until recently, scattering of penetrating energy has limited exploration of the NIR region for medical imaging. Computationally tractable strategies for dealing with scattering, however, have been described [1, 2] and many groups have obtained promising results with media whose optical thickness has clinical significance [1-4].

ii. Contrast: Image quality is a composite of at least five factors: contrast, blur, noise, artifacts, and distortion. Of these contrast is the most fundamental characteristic of an image. Contrast means difference - differences in sensitivity in the patient to the penetrating radiation, that are a consequence of anatomical or physiological variation. The task of imaging is to convert this variation into visual information (*i.e.*, images). Often the contrast naturally occurring is insufficient, and efforts are made to enhance it. Frequently this requires injection of some type of agent. Basically, contrast agents produce their effect either by direct interaction with the penetrating energy (often by absorption, *e.g.*, barium salts in x-ray imaging), or indirectly, by interacting with the surrounding tissue (*e.g.*, gadolinuim lowers the relaxation times in MR). In the case of emissive imaging methods, *e.g.* PET/SPECT, contrast enhancement is achieved by influencing the spatial distribution of the source, either by washout techniques or by use of chelated targeting vehicles. In the NIR region, the sources of contrast are differences in absorption and scattering of near infrared light by different tissues [5-7], and all three contrast enhancement mechanisms are available. This includes use of optical dyes that can absorb the penetrating energy (similar to effect of barium in x-ray imaging), use of fluorescent dyes whose emissivity is influenced by the local chemical environments (similar to gadolinium in MR imaging) and the ability to influence the spatial distribution of the fluorescent probe using washout techniques or targeting vehicles (similar to emission tomography).

iii. Resolution:

Spatial: When seeking information regarding anatomic structures, high spatial resolution is critical. The highest resolution is achieved with x-ray imaging and MR, with resolutions frequently <1 mm. Emission imaging techniques have lower resolution, on the order of 5-10 mm. The principal limitation here is technology. The scintillators in use (NaI) place a lower limit on the area of the detector. Improvements in the form of new higher resolution detectors (under development by some) should produce a corresponding improvement in resolution. Ultimately, resolution will be limited by counting statistics, bowing to the need to limit isotope dosages. The expected limits on spatial resolution for NIR imaging have not been well defined, but most studies suggest that structures on the order of 0.5 cm should be discernible [4, 8, 9]. This value will vary, degrading with increasing depth of the target to the point where photon statistics limit achievable measurements.

Temporal: For the most part, particularly with the primary imaging methods, temporal resolution has not been a feature many have sought to explore. The most basic determinant, is the type of information being sought. For anatomical studies involving non-dynamic tissues, temporal studies have little value. When dynamics are important (*e.g.*, cardiac imaging), the minimum acquisition time in relation to the expected time scale of the temporal variation is limiting.

Often acquisition time is closely tied to the intrinsic sensitivity of the method, which can be limited by the permissible source strength. The last is particularly important for emission tomography, and it is unlikely that these techniques can be adopted to study any fast dynamics, anatomic or otherwise. Fast MRI is becoming available, but limits on intrinsic sensitivity of MR seem likely to limit this to hemoglobin studies. The relatively low x-ray contrast of soft tissues makes this method less desirable for dynamic studies. In other cases, the computational complexity associated with computing multiple images will be limiting. Frequently, both factors are relevant and

dynamic studies invariably require some loss of spatial resolution. The issue of computational complexity will likely remain a factor for some time for possible dynamic studies involving NIR or impedance methods.

iv. Sensitivity: Often the issue of intrinsic measurement sensitivity is not directly considered. Instead it is viewed as a factor that contributes to contrast and resolution. We consider it separately here to make the point that there is a large difference between the intrinsic sensitivity of MR methods and those of other imaging methods, especially those involving isotopic and fluorescence emission. In the case of transmission imaging, (*e.g.*, x-ray, MR) we define sensitivity as the amount of *material* that needs to interact with the penetrating energy in order to produce a measurable change at a surface detector. For emission imaging, we define it as the source strength needed to produce an acceptable S/N ratio within a defined reasonable acquisition time. While MR is a high-resolution method, it is notoriously *insensitive.* Millimole (10^{-3} - 10^{-2}) quantities of material (*i.e.*, molecules containing hydrogen) per voxel are needed to produce good quality images. In contrast, the emission methods are sensitive to picomole quantities or less (10^{-12}), with fluorescence techniques being even more sensitive. Thus, functional imaging studies that seek to detect species in trace quantities will likely remain in the domain of emission tomography.

Table 1 provides a summary of many of the issue discussed above. Row 3 lists the source of contrast for different image modalities. When the inherent tissue characteristics do not produce adequate contrast, it is possible to administer contrast agent, listed in row 4. The contrast agent will alter the contrast characteristics within specific tissues or anatomical regions so that it may enhance the differences between anatomical structures or between normal tissue and lesions. On the other hand, some material may produce unwanted effects that reduce the contrast. This includes background activity, (uncorrected) scattered radiation, septal penetration, etc.

Also listed in Table 1 are the numerical methods used for image recovery. MRI uses the 2-D or 3-D Fourier transform method to convert the composite echo signals in *k*-space to T1 or T2 weighted nucleon density. XCT and ECT uses filtered back-projection or the Fourier slice theorem to reconstruct the CT number and

Table 1. List of properties for different tomographic medical imaging modalities.

Imaging Modality	MRI	XCT (x-ray computed tomography	ECT (SPECT and PET)	Optical Imaging
Penetrating Radiation	Magnetic field and Radio wave (multiples of 40 MHz)	x-ray (bremsstrahlung radiation) from 10 kVp to 150 kVp	γ-ray emitter (*e.g.*, Tc-99m, 140 keV) or positron emitter	near infrared light, i.e., wavelengths from 750 to 1,200 nm
Penetration Properties	low absorption	low absorption low scattering	low absorption low scattering	low absorption high scattering
Source of Contrast	Tissues have different nuclide (H-1, C-13, F-19, Na-23, and P-31) densities, and different T1 and T2	Fat, soft tissue, and bone attenuate x-ray differently	Radionuclides have different affinities for different tissue types and physiological status	Different tissues absorb and scatter near infrared light differently
Contrast Agent	Enhancer: paramagnetic ions (maganese, gadolinium), free radicals	Enhancer: gas, iodine (K edge: 33.2 keV), barium (K edge: 37.4 keV)	Enhancer: antibody	Enhancer: luminescent molecule
Reconstruction	Fourier transform	Backprojection or Fourier slice theory (Radon transform)	Same as CT with attenuation and scattering corrections	Perturbation (Born or iterative Born)
Map	T1 or T2 weighted nucleon density	CT number from reconstructed attenuation coefficients	Concentration of radiopharmaceutical	Absorption or scattering cross sections

radiopharmaceutical concentration, respectively. Basically, the methods adopted vary in their computational complexity in accordance with the uncertainty associated with the path of detected energy. Currently, NIR and impedance methods have the greatest computation burden. While more efficient methods are continuously being developed, it is unlikely that these will have the efficiency seen with the more established imaging methods.

3. NIR Imaging: Scattering Tomography

In this section we turn our attention to specific features associated with NIR imaging. Features favoring practical development are that optical technologies are economical, compact, have low power requirements and can be made portable, unlike the primary imaging methods that require large, costly, fixed installations. In addition, optical methods, especially fluorescence, are well known as among the most sensitive of all analytic techniques. It is useful to compare x-ray and NIR imaging.

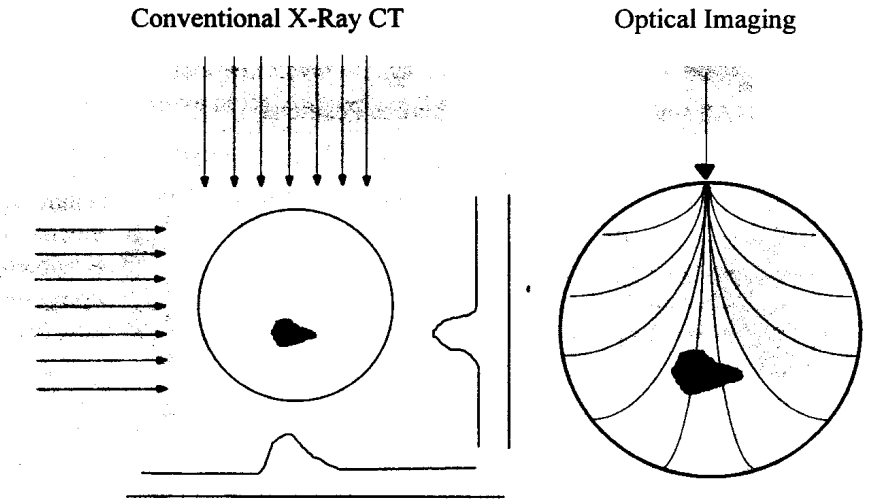

Figure 2. Illustration of difference between photon migration in biological tissue for the x-ray source and a near infrared light source.

As illustrated in Figure 2, x-rays penetrate the object in a straight line manner because photoelectric absorption is the dominant interaction. Near infrared light, on the other hand, is strongly elastically scattered, causing each photon to take a zigzag path and producing spreading of light throughout the object. Scattering complicates the reconstruction for optical tomography because, unlike the x-ray CT, the backprojection algorithm or Fourier slice theorem developed for straight line tomography does not apply. Instead, a more computationally intensive perturbation approach is required. Applicable source conditions include continuous wave (CW), a phase modulation (PM), or a time resolved (TR) waveform. The perturbation method can be solved using any of several well known methods such as the Born approximation [10], iterative Born approximations [11, 12], or Rytov approximation [10] that have also been used in x-ray tomography or microwave imaging. It relates the perturbed detected signal to the perturbation in the absorption or scattering cross section,

$$\mathbf{W}\Delta\mathbf{x} = \Delta\mathbf{I}, \tag{1}$$

where $\Delta\mathbf{x}$ is a vector of absorption or scattering cross section differences between a reference and test medium, $\Delta\mathbf{I}$ is a vector of changes in detector readings between the two media, and $\mathbf{W}$ is a weight matrix describing the influence of each volume element (voxel) on the detector readings. The elements of W are essentially the first partial derivatives of the detector readings with respect to the absorption or scattering coefficients in the reference medium. Different algorithms has been adopted to solve Eq. (1), including iterative algebraic methods (CGD, POCS, SART, ...) and SVD decomposition.

Figure 3 illustrates the quality of computed images achievable using single and multiple (4) DC source positions. The medium contains a single inclusion embedded in a 2D isotropic scattering background. Noteworthy, is that an approximately correct location can be computed in the case of only one source. With four sources, the reconstruction is quite accurate. This illustrates a fundamental difference between the straight line tomography used in XCT and ECT, and the scattering tomography adopted by optical imaging. Image reconstruction by straight-line tomography is simpler and more efficient. Scattering tomography, on the other hand, can derive more information from the detected signal by considering the scattered light, which is usually excluded in straight line tomography.

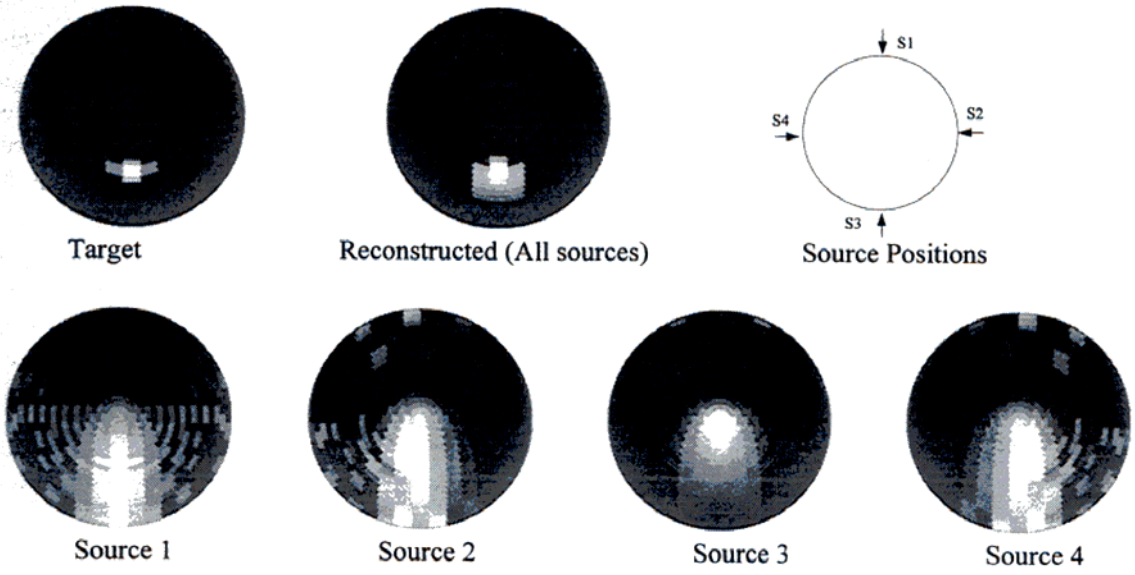

Figure 3. 2-D reconstruction results from detector readings of each individual CW source after 100,000 iterations, using the CGD algorithm with a matrix rescaling technique (rescaling the maximum of each column to 1.

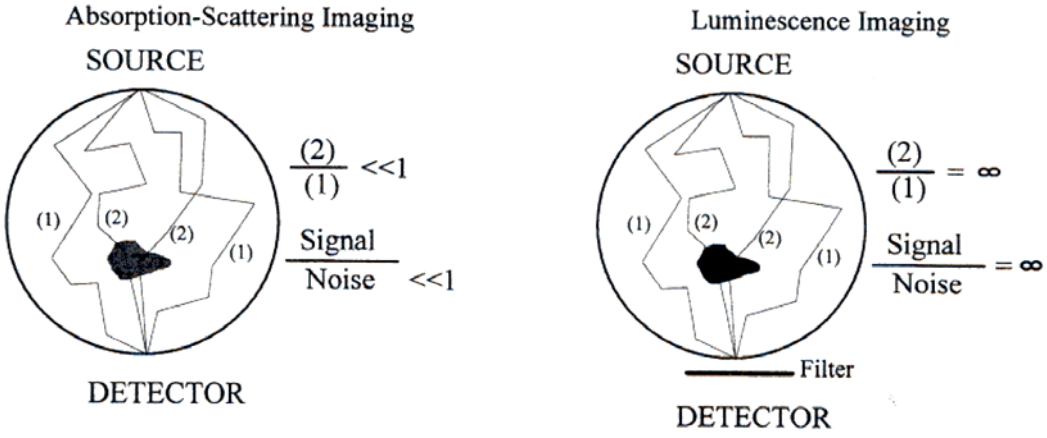

Figure 4. Comparison of absorption-scattering and luminescent imaging.

4. Contrast Enhancement in Optical Tomography - Luminescent Imaging

Radiolabeled and fluorescent–tagged biomolecules have been successfully used in a range of biomedical research studies for many years. Radioisotopes are also widely used in practical medical imaging, *e.g.*, ECT, to provide useful anatomical and physiological information. The use of fluorescent probes in clinical studies has been limited mostly to *in vitro* examination of stained tissue slices. The mean lifetime and quantum yield of many

lumiphores are environmentally sensitive to, for example, oxygen levels, metal ion concentrations, pH, or lipid composition in the near infrared region [13, 14]. Lumiphores conjugatable to larger carrier molecules also are becoming increasingly available. Thus it should also be possible to exploit these sensitivities as a contrast enhancement agent in order to derive useful anatomical and physiological information.

The presence of a lumiphore produces a perturbation of mainly the absorption cross section so that the imaging problem is basically that same as for imaging of scattering and absorption cross sections [8, 15-18]. There is, however, one specific advantage that make luminescent imaging more attractive. That is, lumiphores absorb the excitation photons and emit emission photons at a different wave length. This difference is called the Stokes' shift. One major problem in absorption and scattering imaging is that the perturbed detected readings are much smaller than the reference readings, which can make the perturbed readings sensitive to noise. This obstacle vanishes if the Stokes shift is large enough that a filter can exclude the excitation photons. This idea is illustrated in Figure 4 where "(1)" indicates the reference photons or excitation photons, and "(2)" is the perturbed signal or the emission photons used for reconstruction. It is apparent from Figure 4 that, when an ideal filter is used and completely removes the excitation light, the signal-to-noise ratio can be infinite if other sources of noise are not considered. In reality, ideal filters will never be available, and the presence of other noise sources such as shot noise, quantization error, and additive noise, will reduce this ratio.

Background Lumiphore

Luminescent compounds play a role in optical tomography similar to that of radiopharmaceutical agents in nuclear medicine. In both cases, molecules actively emit photons from which projection or tomographic images are reconstructed. It is well known in nuclear medicine that background activity significantly affects image contrast and image quality [19, 20]. The index usually used in quantitative studies of the background's effect on image quality is the "lesion-to-background" or "target-to-background" uptake or concentration ratio [20]:

$$C_l = (R_l - R_o)/(R_l + R_o + 2R_b) \tag{2}$$

where R_l, R_o, and R_b, respectively are the concentrations in the lesion, object and background, as illustrated in Figure 5. Typically it is desirable to use an agent that yields the highest attainable target-to-background ratio. This index may not be adequate for optical tomography because, unlike x-rays, in nuclear medicine which travel essentially in straight lines, photons in optical tomography are strongly scattered and travel through a much larger volume. Photons collected by a detector encode information about the entire medium, rather than just the thin tube of medium, that is the only portion seen by any one detector in nuclear medicine. Thus, the background index needs to be revised to encompass the contribution to each detector reading of the total *amount* of lumiphore present in the background.

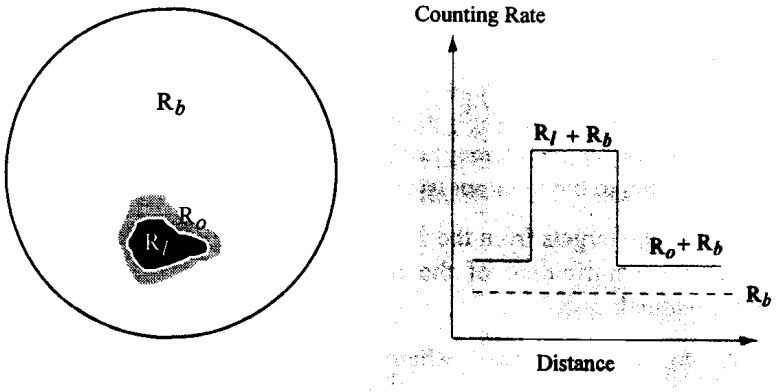

Figure 5. Illustration the quantities used for the definition of background to target ratio of Eq. 2 used in nuclear medicine.

A better definition for the index of the difficulty level caused by the background contribution can be obtained as follows. Using $\mathbf{r}$, $\mathbf{r}_0$, and $\mathbf{r}_s$ as defined in Figure 6, and a diffusion approach [21, 22] to analyze the photon migration, the ratio of contributions from the background and target is approximately

$$\frac{\tilde{R}_B}{\tilde{R}_{tr}} \approx \left(\frac{\gamma \sigma_{T\,1\to 2} N_0 e^{-j\left(k^x|\mathbf{r}_0-\mathbf{r}_s|+k^e|\mathbf{r}_0-\mathbf{r}_d|\right)} e^{-j\tan^{-1}\omega\tau} V_T}{(4\pi)^3 |\mathbf{r}_0-\mathbf{r}_s|^2 |\mathbf{r}_0-\mathbf{r}_d|^2 \sqrt{1+\omega^2\tau^2}} \right)^B_{tr} \tag{3}$$

where k^x and k^e are the complex wave numbers, and V is the total volume of the lumiphore occupied [23]. This ratio is a function of the concentration background–to–target ratio, the location of the target, and the size of the target.

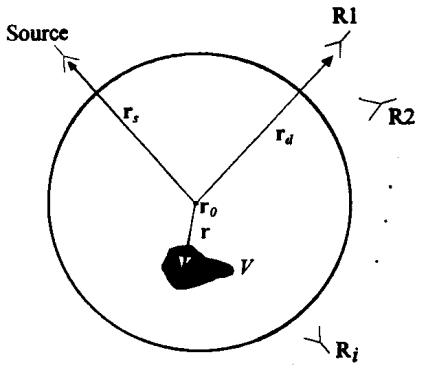

Figure 6. Illustration the quantities used to define the background to target ratio in luminescent imaging.

Improved Reconstruction Algorithm with Concentration Correction

A new procedure was developed to improve the reconstruction of concentration and mean lifetime when background lumiphore is present, by directly estimating the background lumiphore's contribution from the detector readings. We assumed that the background lumiphore is uniformly distributed with a constant concentration and mean lifetime, and that the target is an isolated object. Under these assumptions, the new procedure is:

1. Estimate the background luminescence yield (BLY) via the *maximum possible yield principle* (MPYP). This is a technique to compute a reasonable estimate *bly* of the (true) BLY from the DC detector readings. Suppose that all of the detected signal comes from background lumiphore. Since the BLY is constant, it is equal to the ratio of a detector reading to the corresponding weight function integrated over the entire volume of the medium. An estimate of BLY is obtained for each detector reading, and the lowest of these estimates is used as *bly*. BLY must be ≤ *bly*, since BLY > *bly* would imply negative contributions to the detector readings from the target.

2. Reconstruct $\gamma\sigma_{a,l}N_0$ using an iterative algorithm (*e.g.*, CGD, POCS, SART) with a range constraint, where the upper and lower bounds respectively are the maximum possible target luminescence yield and *bly*. The former is estimated by supposing that all of the lumiphore added to the medium is concentrated in the target volume.

3. Re-estimate the BLY. That is, after reconstructing the targets from the initial *bly*, a new *bly* can be computed for use in the next reconstruction by subtracting the contribution of the reconstructed target from the detector readings. Repeat 1 - 3 until satisfactory *bly* is obtained.

4. Restrict the target volume by setting $\gamma\sigma_{a,l}N_0$ to *bly* in all voxels where $\gamma\sigma_{a,l}N_0 - bly$ is less than a preset fraction of $\max(\gamma\sigma_{a,l}N_0) - bly$.

5. Reconstruct the mean lifetime of the target and background. Here, we sum the weight function over all the background voxels so that the unknowns in this reconstruction are the voxels in the target plus one "lump" background voxel, thereby greatly reducing the dimension of the vector of unknowns.

Results and Discussion

Our earlier report [15, 16] described an algorithm that sequentially computes $\gamma\sigma_{a,l}N_0$ and τ using DC and AC data. In the presence of background lumiphore, however, the original algorithm, which used a positivity constraint, failed to provide accurate quantitative results for either $\gamma\sigma_{a,l}N_0$ or τ (Figure 7). The algorithm set many voxels to zero while reconstructing $\gamma\sigma_{a,l}N_0$, instead of generating the uniform background we expected. It is likely that this is a consequence of the underdeterminedness of the weight matrix, which has infinitely many left–inverses, and that a uniform distribution does not lie on the fastest–converging path chosen by the algorithm. For a fixed target–to–background luminescence yield ratio, more accurate reconstructions were obtained for larger targets. This indicates that the background–to–target lumiphore ratio is not by itself a meaningful index of the difficulty of an image reconstruction problem, and the target size should be considered as well.

The reconstructions shown in Figures 8 and 9, produced by the revised algorithm, show significant improvement over those obtained from the original version, even though the background–to–target lumiphore ratio is twenty times larger in Figure 3 than in Figure 2. The qualitative and quantitative results are better after the third estimate of BLY (Figure 9) than after the first (Figure 8). The correlation of image quality with target size is not significant, or even becomes negative, because the BLY is accurately estimated using the MPYP. The size of the target, however, is underestimated for larger targets, while the quantitative values are overestimated. This is probably a consequence of the underdeterminedness of the weight matrix, and the error can be reduced by using regularization techniques [24, 25]. In addition, the reconstructed mean lifetime is less accurate for larger objects because of the underestimated target size. The negative correlation between image quality and target size seems reasonable when we recall that the presence of a large target increases the detector readings appreciably above that due to the background. Thus, the BLY is overestimated by an amount depending on the target's yield, size and location. High target yields, large targets, and targets located near sources or detectors result in significant overestimates of the BLY, thus distorting the reconstructed images.

The addition of noise distorted the reconstructed images in a noise–level–dependent manner. Results shown in Figure 10 demonstrate that reasonable qualitative accuracy was obtained from the improved algorithm even for 10% Gaussian noise added to the detector readings. The quantitative estimate of $\gamma\sigma_{a,l}N_0$ is inaccurate because of the noise. The mean lifetime values, however, are acceptable for up to 5% noise, even if the quantitative estimate of $\gamma\sigma_{a,l}N_0$ is incorrect. This is reasonable because $\gamma\sigma_{a,l}N_0$ is used only to delineate the target from the background. Its quantitative value is not important, because that is factored out in the mean lifetime reconstruction.

5. Conclusion

Economic pressures are increasingly important in defining the utility of imaging technologies. The primary imaging methods all reside in large, costly, fixed installations. In contrast, optical technologies are compact, economical and can be made portable. In addition, they have the desirable feature of using nonionizing energy sources for which a broad range of chemically sensitive contrast agents can be developed. Development of radioscintigraphic imaging methods has led to establishment of departments of nuclear medicine in many medical centers. As evidenced by results described, it would seem that the foundation for establishing departments of optical medicine may not be far off.

6. Acknowledgements

We acknowledge support from NIH grant RO1–CA59955 and RO1-CA66184-02.

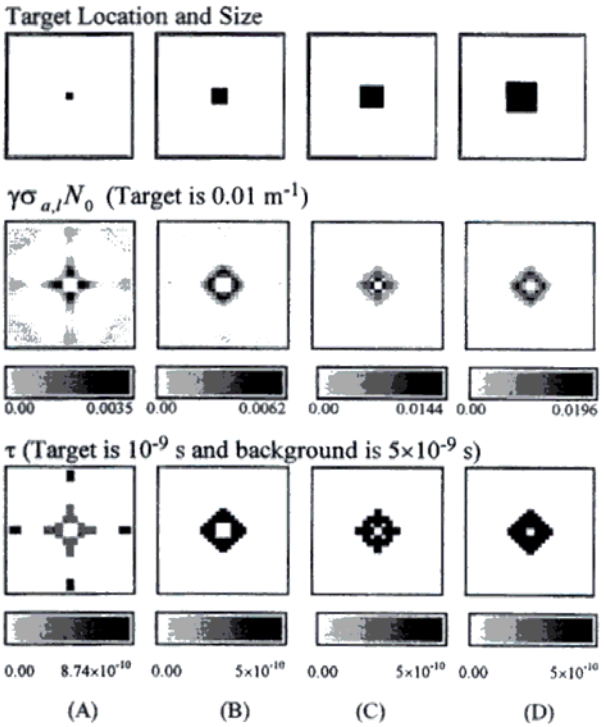

Figure 7. Reconstruction results with background–to–target luminescence yield ratio of 0.01 and different target sizes, using the previously described algorithm [1] with positivity constraints.

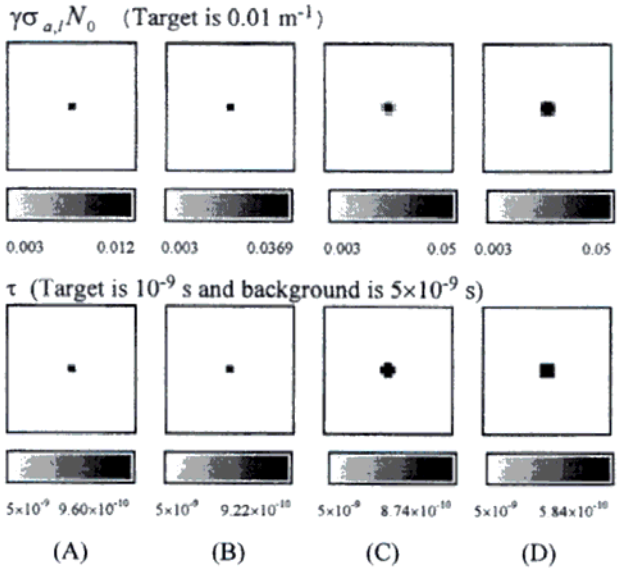

Figure 8. Reconstruction results with background–to–target lumiphore ratio of 0.2 and different target sizes, using the improved algorithm with range constraints, after the first estimate of BLY. Target locations and sizes are the same as for Figure 2, but background–to–target lumiphore ratio is 20 times larger.

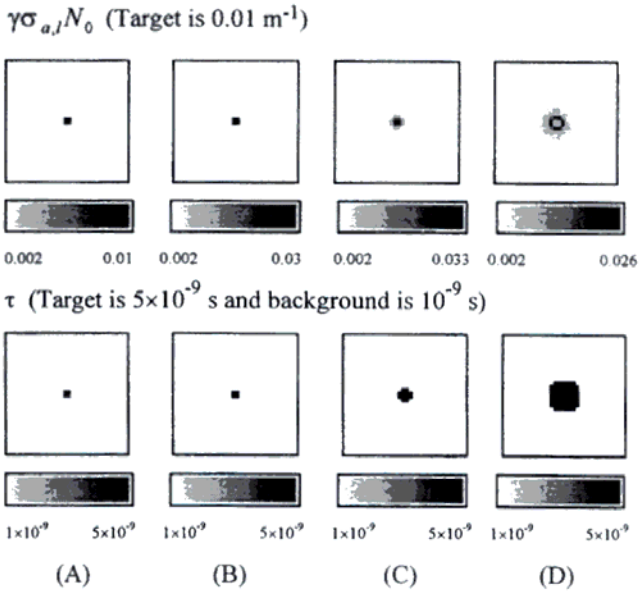

Figure 9. Reconstruction results with background–to–target lumiphore ratio of 0.2 and different target sizes, using the improved algorithm with range constraints and three-step estimate of BLY. Target locations and sizes are the same as for Figure 2.

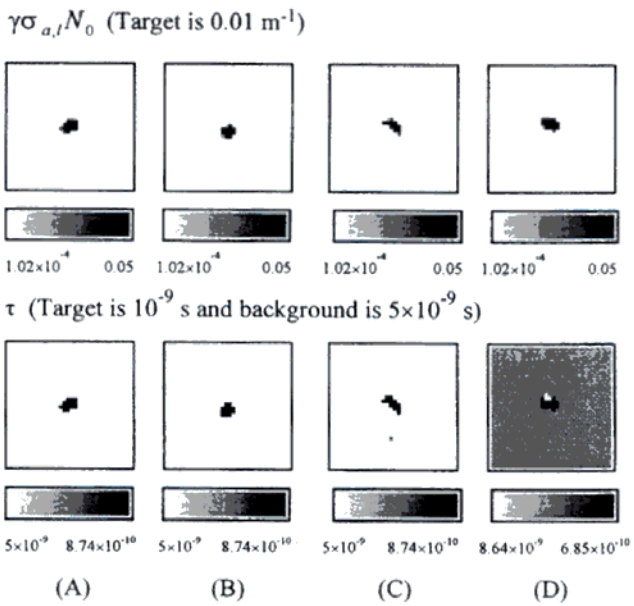

Figure 10. Reconstruction results with background–to–target ratio of 0.01 and different levels of added noise, with target size 2.0 cm×2.0 cm, and using the improved algorithm with range constraints, after the first estimate of BLY. (A) 1.0%, (B) 3.0%, (C) 5.0%, and (D) 10.0% noise

7. References

1. J. Chang, H. Graber, R. L. Barbour, and R. Aronson, "Recovery of optical cross section perturbations in dense scattering media using transport theory based imaging operators and steady–state simulated data and laser measurements," *Applied Optics* , vol. 35, pp. 3963–3978, 1996.
2. S. R. Arridge, "The forward and inverse problems in time resolved infra–red imaging," *Medical Optical Tomography: Functional Imaging and Monitoring*, SPIE Institutes, IS11, pp. 35–64, 1993.
3. M. A. O'Leary, D. A. Boas, B. Chance, and A. G. Yodh, "Experimental images of heterogeneous turbid media by frequency–domain diffusing–photon tomography," *Optics Letters*, vol. 20, pp. 426–428, 1995.
4. H. Jiang, K. D. Paulsen, U. L. Österberg, and M. S. Patterson, "Frequency–domain optical image reconstruction in turbid media: an experimental study of single–target detectability," *Applied Optics*, vol. 36, pp. 52–63, 1997.
5. O. W. van Assendelft, *Spectrophotometry of Haemoglobin Derivatives*, Charles C Thomas, Springfield, IL, 1970.
6. F. A. Duck, *Physical Properties of Tissues*. Academic Press Inc., San Diego, 1990.
7. W.-F. Cheong, S. A. Prahl, and A. J. Welch, "A review of the optical properties of biological tissues," *IEEE J. Quantum Electronics*, vol. 26, pp. 2166-2185, 1990.
8. M. A. O'Leary, D. A. Boas, X. D. Li, B. Chance, and A. G. Yodh, "Fluorescence lifetime imaging in turbid media," *Optics Letters*, vol. 21, pp. 158–160, 1996.
9. J. Chang, H. L. Graber, P. C. Koo, R. Aronson, S.-L. S. Barbour, and R. L. Barbour, "Optical imaging of anatomical maps derived from magnetic resonance images using time-independent optical sources," *IEEE Trans. Medical Imaging*, vol. 16, pp. 68-77, 1997.
10. A. V. Kak and M. Slaney, *Principles of Computerized Tomographic Imaging*. IEEE Press, New York, NY, 1988.
11. Y. M. Wang and W. C. Chew, "An iterative solution of the two–dimensional electromagnetic inverse scattering problem," *Int'l J. Imag. Syst. & Tech.*, vol. 1, pp. 100–108, 1989.
12. W. C. Chew and Y. M. Wang, "Reconstruction of two–dimensional permittivity distribution using the distorted Born iterative method," *IEEE Trans. Med. Imag.*, vol. 9, pp. 218–225, 1990.
13. J. R. Lakowicz, *Principles of Fluorescence Spectroscopy*. Plenum Press, New York, 1983.
14. D. B. Shealy, M. Lipowska, J. Lipowski, N. Narayanan, S. Sutter, L. Strekowski, G. Patonay, "Synthesis, chromatographic separation, and characterization of near-infrared-labeled DNA oligomers for use in DNA sequencing," *Analytical Chemistry*, vol. 67, pp. 247–251, 1995.
15. J. Chang, H. L. Graber, and R. L. Barbour, "Luminescence optical tomography of dense scattering media," *J. Opt. Soc. Am. A*, vol. 14, pp. 288–299, 1997.
16. J. Chang, H. L. Graber, and R. L. Barbour, "Imaging of fluorescence in highly scattering media," *IEEE Trans. Biomed. Eng.*, vol. 44, pp. 810-822, 1997.
17. Y. Paithankar, A. U. Chen, B. W. Pogue, M. S. Patterson, and E. M. Sevick–Muraca, "Imaging of fluorescent yield and lifetime from multiply scattered light reemitted from random media," *Applied Optics*, vol. 36, pp. 2260-2272, 1997.
18. J. Wu, Y. Wang, L. Perelman, I. Itzkan, R. R. Dasari, and M. S. Feld, "Three-dimensional imaging of objects embedded in turbid media with fluorescence and Raman spectroscopy," *Applied Optics*, vol. 34, pp. 3425-3430, 1995.
19. P. Sprawls, Jr., *Physical Principles of Medical Imaging*. Medical Physics Publishing, Madison, Wisconsin, 1995.
20. J. A. Soreneon and M. E. Phelps, *Physics of Nuclear Medicine*, 2nd Ed. W. B. Saunders Company, Philadelphia, Pennsylvania, 1987.

21. A. Ishimaru, *Wave Propagation and Scattering in Random Media*. Academic Press, New York, NY, 1978.

22. J. Lamarsh, *Introduction. to Nuclear Reactor Theory*. Addison–Wesley, Reading, MA, 1966.

23. J. Chang, H. L. Graber, and R. L. Barbour, "Concentration, size, mean lifetime, and noise effect on image quality in luminescence optical tomography," in *Proceedings Optical Tomography and Spectroscopy of Tissue: Theory, Instrumentation, Model, and Human Studies II*, vol. SPIE–2979, pp. 750-758,1997.

24. J. Chang, W. Zhu, Y. Wang, H. L. Graber, and R. L. Barbour, "A regularized progressive expansion algorithm for recovery of scattering media from time–resolved data," *J. Opt. Soc. Am. A*, vol. 14, pp. 306–312, 1997.

25. S. R. Arridge, P. van der Zee, M. Cope, and D. T. Delpy, "Reconstruction methods for infrared absorption imaging," in *Proceedings of Time–Resolved Spectroscopy and Imaging of Tissues*, vol. SPIE–1431, pp. 204–215, 1991.